

CREEP FATIGUE LIFE PREDICTION FOR ENGINE HOT SECTION
MATERIALS (ISOTROPIC) - FOURTH YEAR PROGRESS REVIEW*

Richard S. Nelson and John F. Schoendorf
United Technologies Corporation
Pratt & Whitney

INTRODUCTION

As gas turbine technology continues to advance, the need for advanced life prediction methods for hot section components is becoming more and more evident. The complex local strain and temperature histories at critical locations must be accurately interpreted to account for the effects of various damage mechanisms (such as fatigue, creep, and oxidation) and their possible interactions. As part of the overall NASA HOST effort, this program is designed to investigate these fundamental damage processes, identify modeling strategies, and develop practical models which can be used to guide the early design and development of new engines and to increase the durability of existing engines.

This contract has recently been modified to be a 6-year effort, comprising a 2-year base program and a 4-year option program. Two different isotropic materials (B1900+Hf and INCO 718) will be utilized, along with two protective coating systems (overlay and diffusion aluminide). The base program (ref. 1), which was completed during 1984, included comparison and evaluation of several popular high-temperature life prediction approaches as applied to continuously cycled isothermal specimen tests. The optional program, of which two years have been completed, is designed to develop models which can account for complex cycles and loadings, such as thermomechanical cycling, cumulative damage, multiaxial stress/strain states, and environmental effects.

THERMOMECHANICAL MODEL DEVELOPMENT

A significant task under the optional program is the development of a damage model which is valid under conditions of thermomechanical fatigue (TMF). A total of 32 uncoated and 9 NiCoCrAlY overlay coated TMF specimen tests have been completed so far, covering variables such as strain range, temperature range, mean strain, cycle type, and hold times. Some of the non-standard cycle types used (such as elliptical and dogleg cycles) have demonstrated that TMF damage cannot always be predicted in the same manner as isothermal tests; the chosen model must be sensitive to accumulation of damage from several different sources throughout the cycle.

Six fully reversed TMF specimen tests have been completed at two nominal strain ranges, using both in-phase and out-of-phase cycling. The temperature range was 538-871°C. (1000-1600°F.), and the rate was 1 CPM. A plot of initiation life vs. total mechanical strain range is shown in figure 1, along with median life data from isothermal baseline tests at the same cyclic rate. As expected, the TMF results are lower in life than isothermal data from even the maximum cycle temperature. Note also that the difference in life between in-phase and out-of-phase cycling is a function of strain range; at lower strain ranges, the in-phase cycling produces higher life, while at the higher levels, the out-of-phase life is higher. Obviously, the number of data points in this set is limited, but this behavior has also been

*Work done under NASA Contract NAS3-23288

noted during other TMF testing. This serves to emphasize the need to understand and model the actual damage mechanisms active under these conditions; simple data correlations based on one or the other cycle type may not always give conservative predictions.

In order to provide insight into the relationship between mean strain and TMF life, a series of 7 tests was completed using one-way strain cycling. Five of these tests were run at $R=0$ conditions, and two were run using $R=-\infty$. Figure 2 shows a comparison between the results of the one-way tests and the fully reversed TMF data for out-of-phase cycling. The ordering of the life curves follows the expected trend, with the $R=0$ tests producing the lowest lives and the $R=-\infty$ being the highest. However, as shown in figure 3, the $R=0$, in-phase tests showed no significant difference relative to the fully reversed in-phase tests; in fact, they appeared to be slightly higher in life. This may be due to inherent scatter in the limited data set, or it may be caused by competing damage mechanisms.

The dogleg TMF test (rapid strain cycling at minimum or maximum temperature, followed by strain hold in tension or compression during thermal cycling), was conceived as an intermediate step between an isothermal hold test and a traditional TMF test. Six specimens were tested using such cycles, and their initiation lives are shown plotted on figure 4 along with comparable isothermal and TMF (in-phase and out-of-phase) median test results. The dogleg tests with the hold in compression ("LC" & "HC") are about 2X higher in initiation life than the isothermal compression hold tests. However, the lives from the tension hold dogleg tests ("LT" & "HT") are nearly four times lower than those of similar isothermal tests. By using the median lives from the in-phase and out-of-phase TMF tests, the solid trend line shown on this figure can be drawn, and it is obviously opposite to what was found during the isothermal testing. It is therefore clear that the non-isothermal hold has a significant influence on specimen life, no doubt by activating different damage mechanisms as the temperature varies.

Perhaps the most interesting results obtained so far under this task are those from the elliptical cycle tests (strain and temperature are sinusoidal with time and shifted in phase by ± 135 degrees). Eight specimen tests were completed under this series, including both clockwise (CW) and counterclockwise (CCW) cycles. The CCW cycle is a good simulation of the strain-temperature history experienced by many actual hot section components. Although there are some components which have a CW movement around their strain-temperature history, the CW cycle results are most valuable when compared to the CCW results; the only apparent difference is the direction of motion around the loop. Figure 5 shows a plot of the elliptical test results, and it is clear that there is a large life difference between the two types of cycles. Note that life prediction methods based solely on the extremes of the cycle will not be able to predict this behavior, since they cannot distinguish between these two cycles. To account for such cycle dependent effects, an advanced incremental form of the CDA life prediction model is under development which can be integrated around any arbitrary strain-temperature history curve. This model is undergoing evaluation and refinement at the present time.

MULTI-AXIAL STRESS STATE MODEL

Another of the optional tasks is the development and verification of a multi-axial stress state creep-fatigue life prediction model. A fatigue test program which consists of 26 isothermal strain controlled tests utilizing B1900+Hf thin-walled tubular specimens is being conducted to provide crack initiation data. Four types

of strain cycles are employed in the tests: simple tension, simple torsion, combined tension-torsion in-phase (proportional loading) and combined tension-torsion 90° out-of-phase (non-proportional loading). The torsion to tension strain ratio in the combined strain tests is 1.5. The idealized strain paths in $\epsilon - \gamma$ space for these cycles are shown in figure 6. Two temperature levels, 871°C (1600°F) and 538°C (1000°F), and two frequency levels, 10 CPM and 1 CPM, are being investigated to determine their effect on the cracking behavior and possible changes in stress state dependence. The variation in fatigue life with strain range is also being investigated.

To date, a total of 16 multiaxial specimen tests have been completed. The results are presented in Table I. The tensile test results are similar to those obtained on solid cast uniaxial specimens tested in the base program. This demonstrates the capability of producing consistent fatigue data with the multiaxial test rig and specimen.

Multiaxial fatigue theories that relate to the physical damage processes have shown promise. Therefore, the resultant physical damage has been studied closely by monitoring fatigue crack initiation and growth during test through the use of cellulose acetate surface replicas and by post-test fractographic analysis. These observations indicate that for this material, multiaxial fatigue cracks initiate and grow mainly on planes perpendicular to the maximum normal strain under all loading conditions although some crack growth along maximum shear planes occurs at 538°C (1000°F). Therefore, a single parameter that is consistent with the cracking mode, maximum normal strain, has been used to correlate the test results (figure 7). It can be seen that there is considerable overall scatter in the two temperature groupings of data, but the results for the four strain cycles are intermingled. Other investigators (ref. 2) have consistently found out-of-phase tension-torsion loading to be more damaging, especially with a 90° phase angle, than in-phase loading. Damage from non-proportional loading may depend on a number of variables such as material, temperature level and strain amplitude and, therefore, may be difficult to characterize. Metallographic observations indicate that extensive rubbing of opposing fracture surface features occurred during the 90° out-of-phase tension-torsion tests; examinations of these specimens by SEM have not provided useful information concerning the crack initiation sites.

Trial data correlations have also been accomplished using other potential multiaxial fatigue parameters such as equivalent strain, maximum shear strain and plastic work per cycle (ref. 3) with limited success. None of the parameters produced an acceptable correlation of the test data, due in part to their inability to properly account for the pure torsion tests which resulted in significantly higher fatigue lives. In addition, during the determination of the plastic work, the hysteresis loops for B1900+Hf exhibited little plasticity even for fatigue tests that resulted in fairly low lives, as shown in figure 8. This situation caused plastic work calculations to be very critical, and fatigue life assessment to be extremely sensitive to small changes in experimental measurements or analytical calculations of cycle plasticity.

Part of the scatter in the data is due to the low life of the in-phase tension-torsion test of specimen 204 which may have been adversely affected by dross found at the initiation site (figure 9). Subsequent to this discovery, an inspection program was undertaken to screen 22 untested specimens using X-ray, fluorescent penetrant and visual inspection procedures. Although indications of minor subsurface shrinkage were found in most of the specimens, no surface or subsurface discontinuities were discovered that would disqualify these specimens.

Work is continuing to complete the 10 remaining specimen tests. Additional single and multiple parameters will be investigated to characterize the multiaxial fatigue behavior.

CUMULATIVE LOADING MODEL

Work under this task has been completed during the past year, based on the results of a total of 50 cumulative damage tests. These include block tests (one set of conditions for the first block of cycles, followed by a second set of conditions for the remainder), sequenced tests (alternating blocks of two different sets of conditions), and interrupted tests (fatigue cycling interrupted by periods of temperature exposure, either with or without load). The results of these tests show that some conditions obey a linear damage rule, while certain other conditions show a strong non-linear interaction. The non-linear damage accumulation method and the ductility fraction concept which were discussed at last year's workshop have been incorporated into the formulation of the CDA model to account for the observed interaction effects. It is expected that future refinements of these equations will continue to be made until the end of the optional program.

ENVIRONMENTAL ATTACK MODEL

An environmental creep-fatigue test program which consists of 27 tests utilizing B1900+Hf solid smooth baseline fatigue specimens has been determined for this optional task. Isothermal, fully reversed, strain controlled tests will be conducted in inert argon, in oxygen at partial pressures typical of that encountered in the engine hot section, and in laboratory air. The crack initiation results will be used to develop, evaluate and verify a model for prediction of environmental (oxidation) effects on the creep-fatigue life.

Test results from previous tasks were reviewed to determine test conditions that would activate the various damage processes, including oxidation. The program incorporates two temperature levels, 982°C (1800°F) and 871°C (1600°F), and two strain rates, $1.67 \times 10^{-3} \text{ sec}^{-1}$ and $1.67 \times 10^{-4} \text{ sec}^{-1}$. Testing will be done in two stages: 1) screening tests will be run to determine the alternative environment (inert argon or pressurized oxygen) with the greatest effect, and 2) utilizing this alternative environment in conjunction with laboratory air by varying the length and order of exposure to demonstrate the effects of the environment at different stages in the development of a fatigue crack.

A stainless steel, low pressure test chamber (figure 10) has been designed and built to accommodate the planned environmental tests. The chamber has been subjected to an overpressure test which demonstrated its capability to withstand a maximum pressure at least 2X greater than the working pressure of 5 atmospheres.

The initial environmental experiments are scheduled to begin shortly using a test rig that is now being outfitted with the pressure chamber and other necessary accessories.

PROTECTIVE COATINGS MODELS

Under the modified version of this task, a total of 8 overlay coated specimens will be tested. Two such tests have been completed using one-way strain cycling: one at 1600°F and 10 CPM, and one at 1800°F and 1 CPM. The 1600°F test showed a significant increase in initiation life when compared to similar tests on uncoated specimens, but the separation life was essentially the same. However, the test which was

run at 1800°F showed approximately a 3X increase in both initiation and separation lives over the uncoated results.

CYCLIC MEAN STRESS MODEL

A total of 25 controlled mean stress tests are planned for this task, including five under TMF conditions. Two of these TMF tests have been completed using load control to achieve the desired mean stress. The mean stresses chosen were +30 and +10 KSI, and the resulting mean strain histories of these specimens are shown in figure 11. It can be inferred that a significant amount of creep damage occurred during these tests, and it is therefore not surprising that the lives were significantly reduced relative to strain controlled testing (by a factor of 40X for the +30 KSI test). The isothermal portion of this testing will be conducted at the University of Rhode Island by Professor Ghonem.

ALTERNATE MATERIAL TESTING

A rolled ring forging of AMS 5663 (INCO 718) material has been obtained for use in this portion of the program. A total of 70 isothermal tests (both monotonic and fatigue), 20 TMF tests, and 15 multiaxial tests are currently planned as part of this task. Machining of these specimens is well underway, and testing is scheduled to begin in the last quarter of 1986.

FUTURE TASKS

Further work is continuing on all the above tasks, with a view to producing a creep-fatigue model which is both practical and accurate. During the coming year, the focus of the efforts is planned to shift from generation of test data to analytical model development activities. The generation of CDA model constants for INCO 718 will be completed first, followed by additional refinement of the CDA life prediction model.

REFERENCES:

1. Moreno, V., Nissley, D. M., and Lin, L. S., " Creep Fatigue Life Prediction for Engine Hot Section Materials (Isotropic) - Second Annual Report," NASA CR-174844, March 1985.
2. Kanazawa, K., Miller, K.J. and Brown, M.W., "Low-Cycle Fatigue Under Out-of-Phase Loading Conditions", ASME Journal of Engineering Materials and Technology, Vol. 99, No. 3, July 1977, pp. 222-228.
3. Garud, Y.S., "A New Approach to the Evaluation of Fatigue Under Multiaxial Loadings, " ASME Journal of Engineering Materials and Technology, Vol. 103, April 1981, pp. 118-125.

TABLE I
MULTIAXIAL FATIGUE TEST RESULTS

Specimen Number	Temp. (°F)	Freq. (CPM)	$\Delta\epsilon$ (%)	$\Delta\gamma$ (%)	Phase Angle (Deg.)	Crack Initiation Life* (Cycles)
217	1600 ↓	10.0 ↓	<u>+0.250</u>	0.0	-	1150
222			<u>+0.200</u>	0.0	-	14,600
203			0.0	<u>+0.404</u>	-	8100
219			0.0	<u>+0.361</u>	-	40,000
204			<u>+0.185</u>	<u>+0.260</u>	0	350
218			<u>+0.147</u>	<u>+0.220</u>	0	6900
216			<u>+0.250</u>	<u>+0.375</u>	90	1250
205			<u>+0.147</u>	<u>+0.220</u>	90	11,700
220			<u>+0.338</u>	0.0	-	1950
201			<u>+0.260</u>	0.0	-	4100
221	1000 ↓	1.0 ↓	0.0	<u>+0.675</u>	-	1350
209			0.0	<u>+0.500</u>	-	20,100
223			<u>+0.255</u>	<u>+0.382</u>	0	2200
202			<u>+0.338</u>	<u>+0.506</u>	90	240
214			<u>+0.250</u>	<u>+0.375</u>	90	6100
215			<u>+0.338</u>	<u>+0.506</u>	90	500

*These lives are preliminary and subject to change as additional inspection data become available.

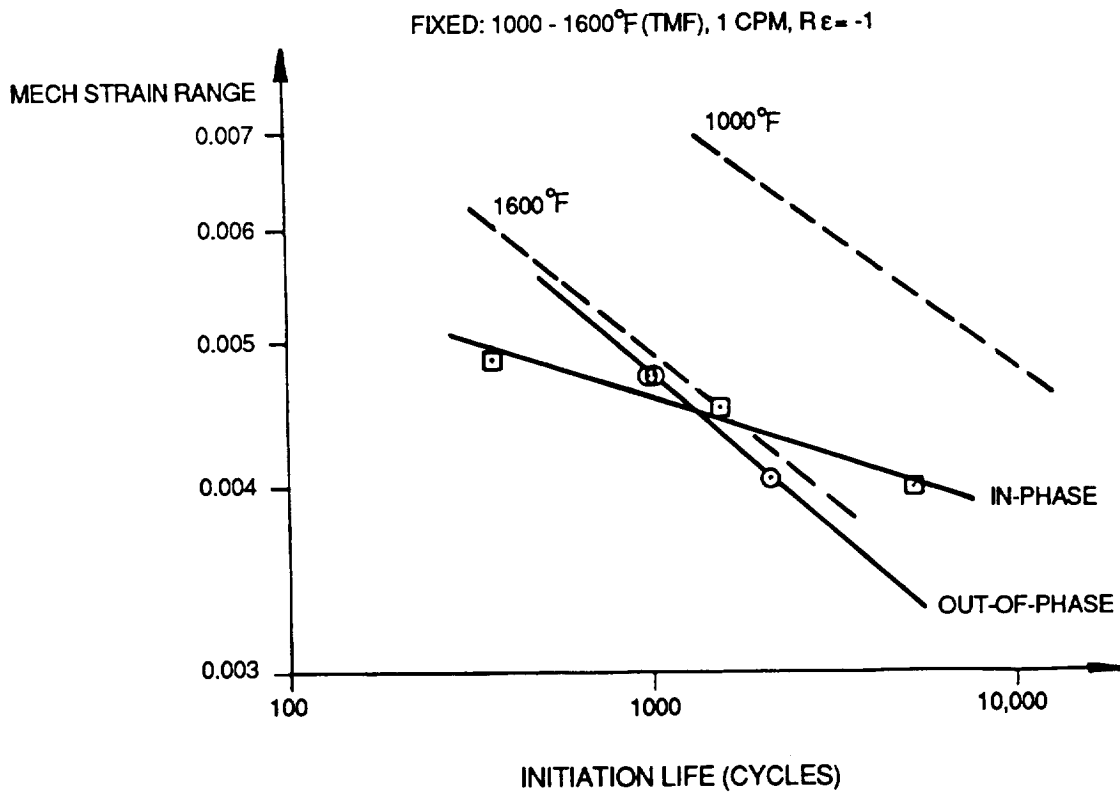


Figure 1 TMF Test Results for In-Phase and Out-of-Phase Cycles

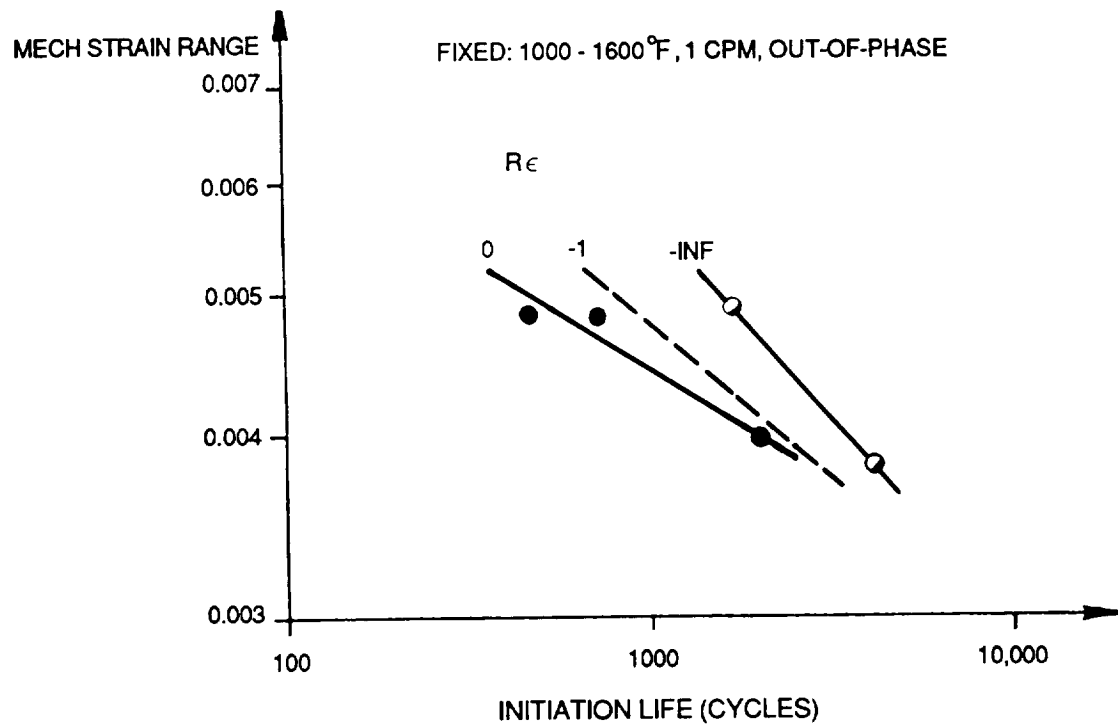


Figure 2 Strain Ratio Effect on Out-of-Phase TMF Tests

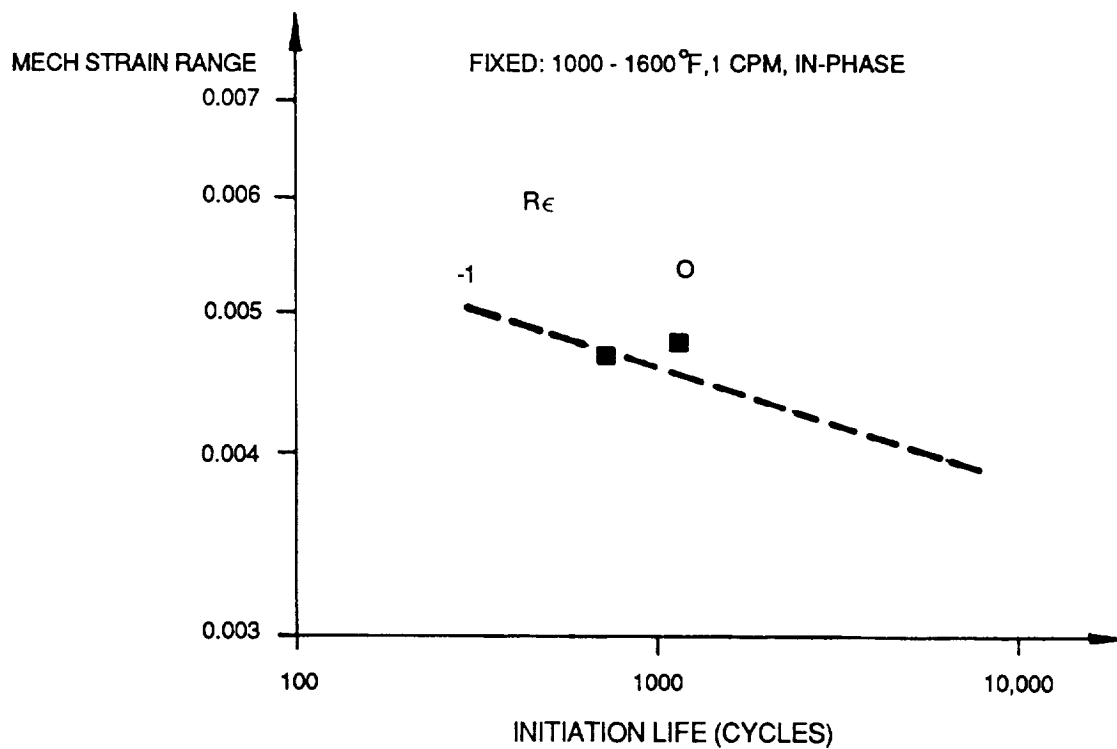


Figure 3 Strain Ratio Effect on In-Phase TMF Tests

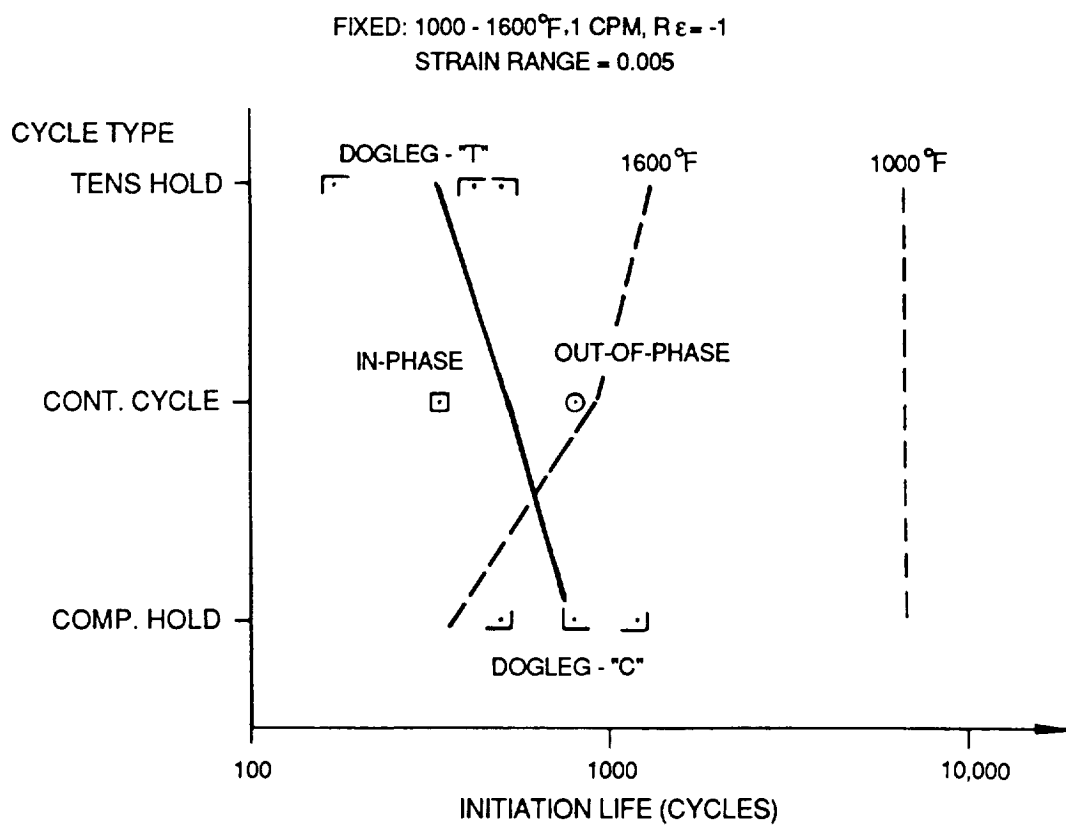


Figure 4 Dogleg TMF Test Results

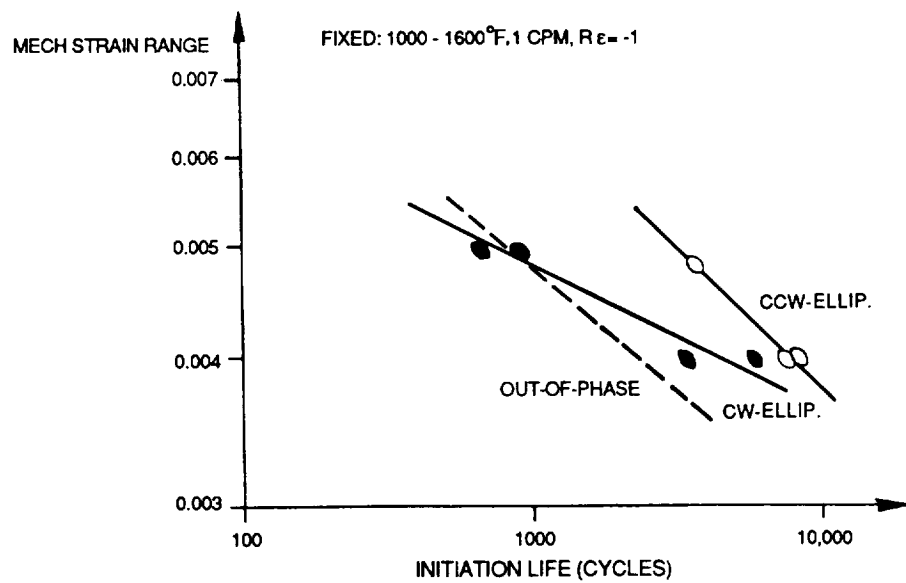


Figure 5 Elliptical Cycle TMF Test Results

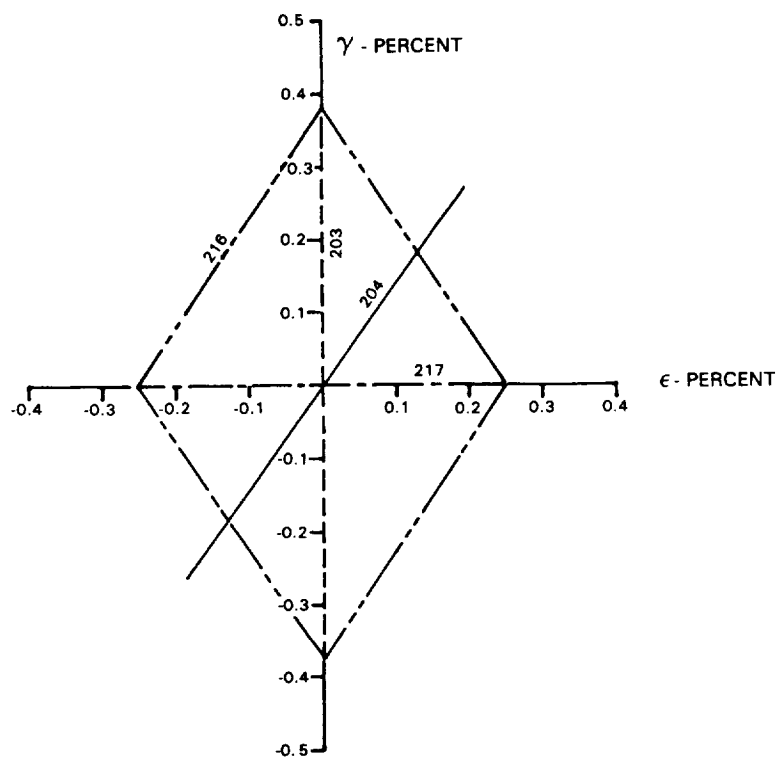


Figure 6 Multiaxial Test Specimen Strain Paths

ORIGINAL PAGE IS
OF POOR QUALITY

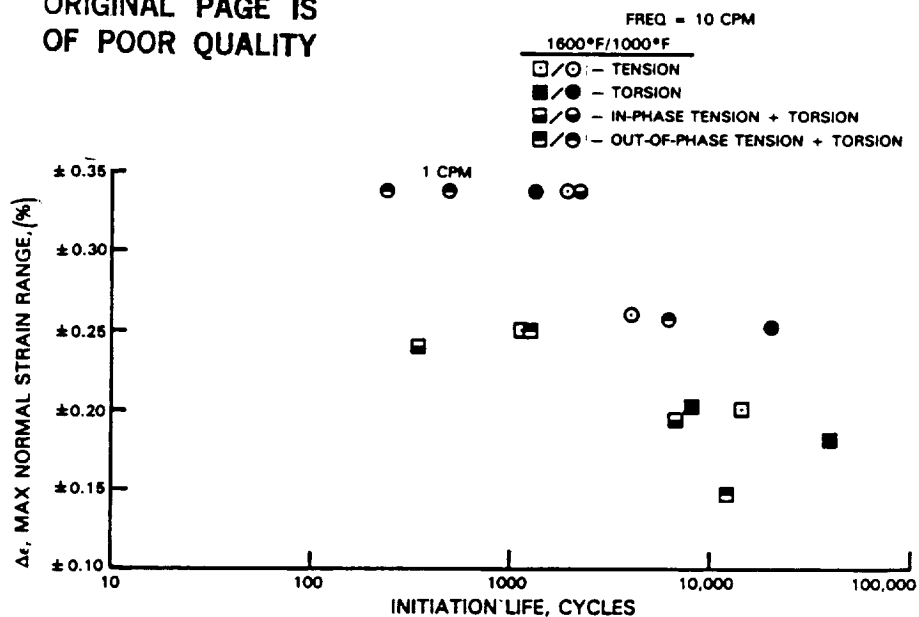


Figure 7 Maximum Normal Strain Range Versus Crack Initiation Life

SPECIMEN 216
TENSION-TORSION 90° OUT-OF-PHASE

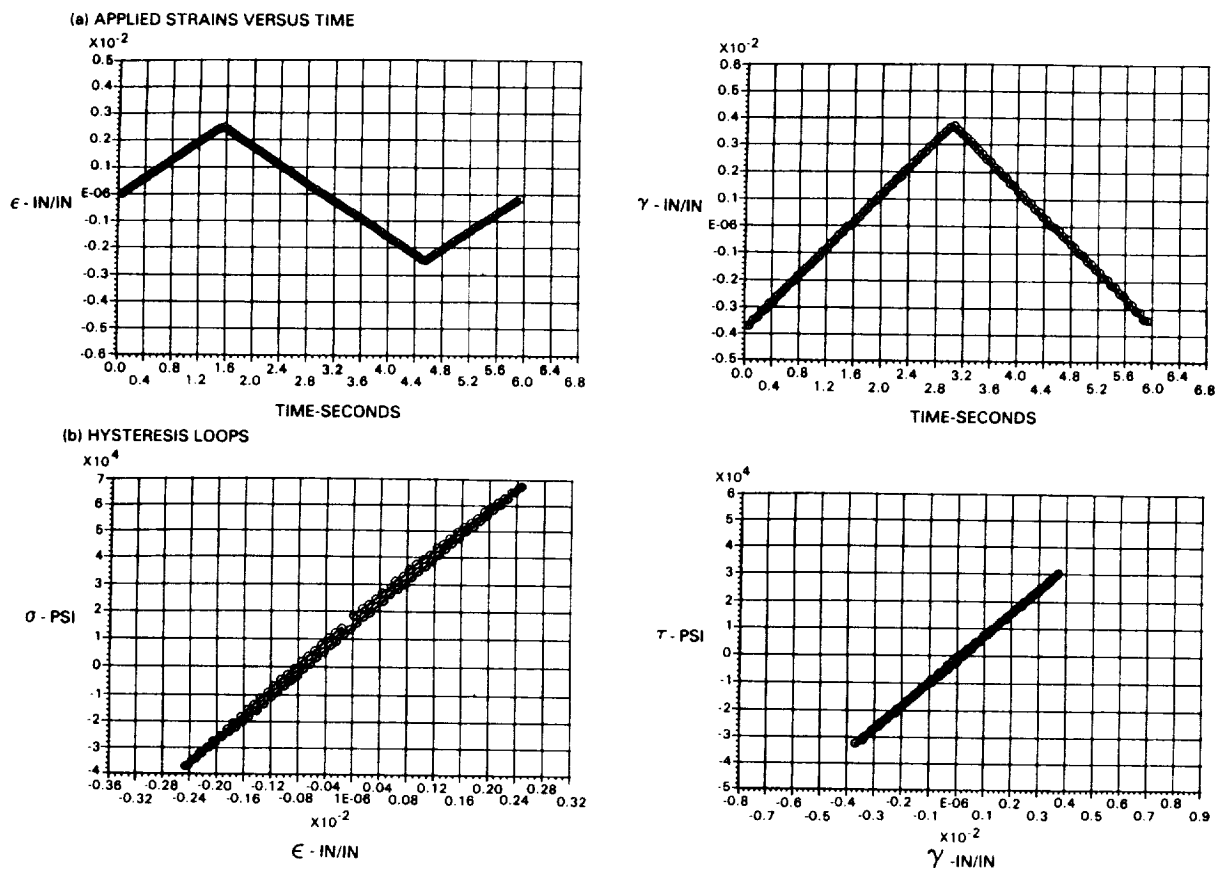
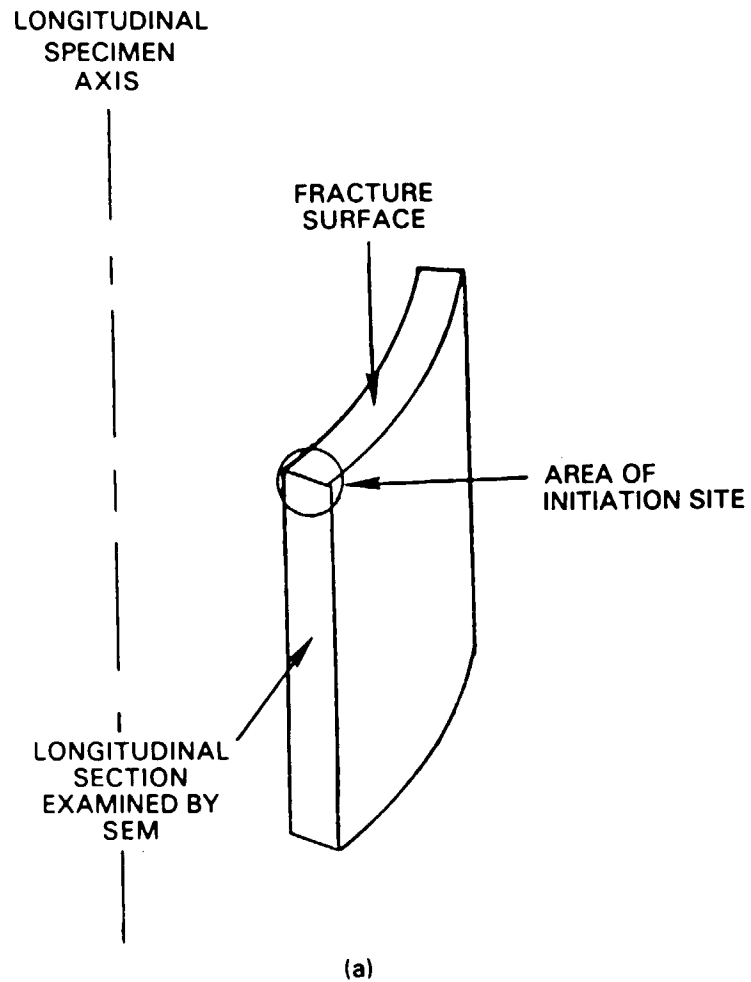


Figure 8 Specimen 216 Tension-Torsion 90° Out-of-Phase



OF FOUR QUALITY

Figure 9 Characterization of longitudinal section through initiation site.

- (a) Schematic diagram showing orientation of section examined by SEM.
- (b) SEM micrograph of longitudinal section at initiation site showing oxide buildup on fracture surface as well as in secondary crack.

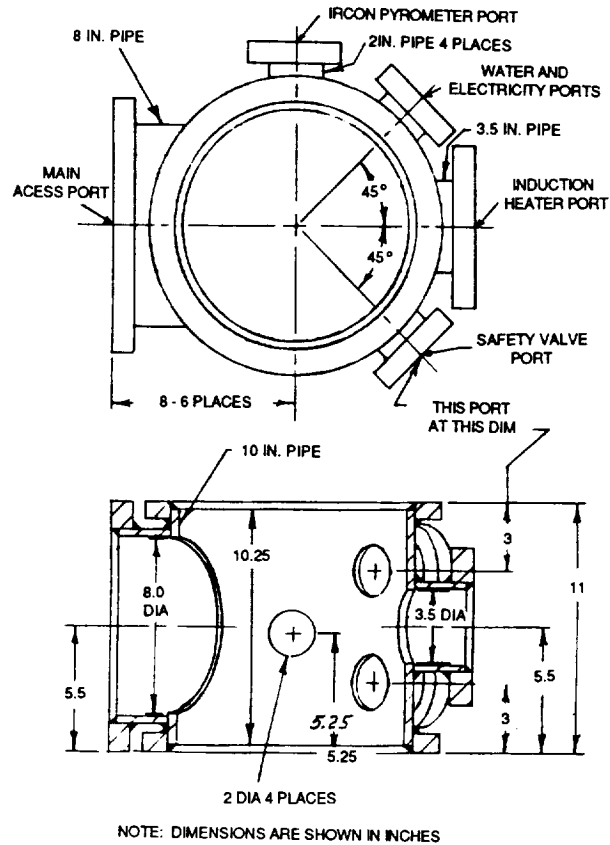


Figure 10 Environmental Test Chamber

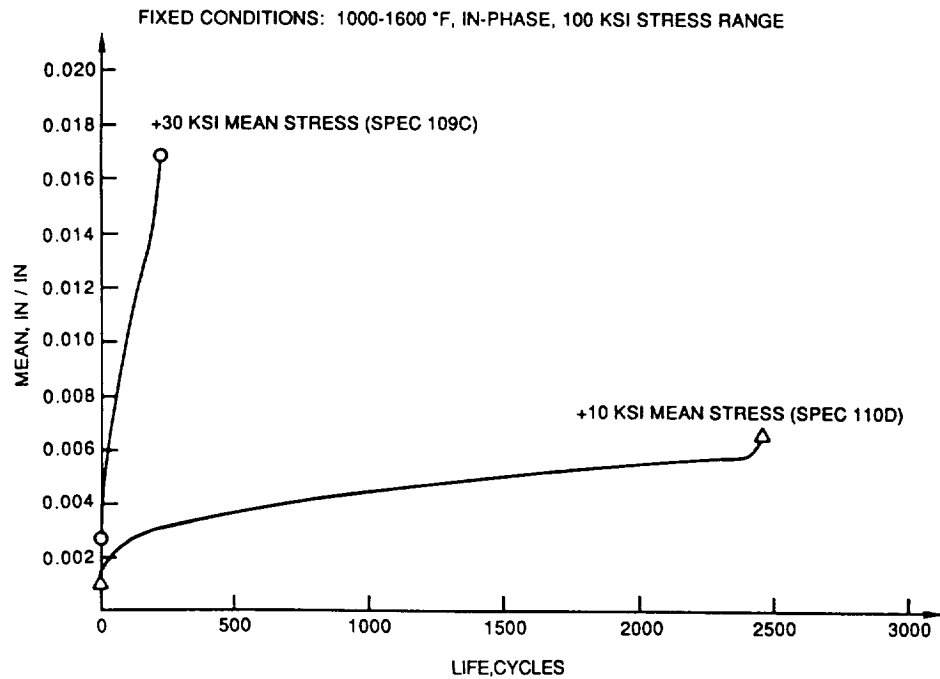


Figure 11 Mean Strain History for Controlled Mean Stress TMF